Coexistence of a pseudogap and a superconducting gap for the high-T_{c} superconductor La_{2−x}Sr_{x}CuO_{4} studied by angle-resolved photoemission spectroscopy

T. Yoshida, W. Malaeb, S. Ideta, D. H. Lu, R. G. Moor, Z.-X. Shen, M. Okawa, T. Kiss, K. Ishizaka, S. Shin, Seiki Komiya, Yoichi Ando, H. Eisaki, S. Uchida, and A. Fujimori

Phys. Rev. B **93**, 014513 — Published 19 January 2016

DOI: 10.1103/PhysRevB.93.014513

Coexisting pseudo-gap and superconducting gap in the high-T_c superconductor $La_{2-x}Sr_xCuO_4$

T. Yoshida[1], W. Malaeb[1], S. Ideta[1], D. H. Lu[2], R. G. Moor[2], Z.-X. Shen[2], M. Okawa[3], T. Kiss[3], K. Ishizaka[3], S. Shin[3], Seiki Komiya[4], Yoichi Ando[5], H. Eisaki[6], S. Uchida[1], A. Fujimori[1]

[1]*Department of Physics, University of Tokyo, Bunkyo-ku, Tokyo 113-0033, Japan*

[2]*Department of Applied Physics and Stanford Synchrotron Radiation Laboratory, Stanford University, Stanford, CA94305*

[3]*Institute of Solid State Physics, University of Tokyo, Kashiwa 277-8581, Japan*

[4]*Central Research Institute of Electric Power Industry, Yokosuka, Kanagawa 240-0196, Japan*

[5]*Institute of Scientific and Industrial Research, Osaka University, Ibaraki, Osaka 567-0047, Japan and*

[6]*National Institute of Advanced Industrial Science and Technology, Tsukuba 305-8568, Japan*

(Dated: December 21, 2015)

Abstract

Relationship between the superconducting gap and the pseudogap has been the subject of controversies. In order to clarify this issue, we have studied the superconducting gap and pseudogap of the high-T_c superconductor $La_{2-x}Sr_xCuO_4$ (x=0.10, 14) by angle-resolved photoemission spectroscopy (ARPES). Through the analysis of the ARPES spectra above and below T_c, we have identified a superconducting coherence peak even in the anti-nodal region on top of the pseudogap of a larger energy scale. The superconducting peak energy nearly follows the pure d-wave form. The d-wave order parameter Δ_0 [defined by $\Delta(k) = \Delta_0(\cos k_x a - \cos k_y a)$] for x=0.10 and 0.14 are nearly the same, Δ_0 ∼12-14 meV, leading to strong coupling $2\Delta_0/k_BT_c \sim 10$. The present result indicates that the pseudogap and the superconducting gap are distinct phenomena and can be described by the "two-gap" scenario.

PACS numbers: 74.25.Jb, 71.18.+y, 74.70.-b, 79.60.-i

In the studies of the high-T_c cuprates, it has been a long-standing issue whether the pseudogap is related to the superconductivity or a phenomenon distinct from the superconductivity. Preformed Cooper pairs lacking phase coherence[1] or superconducting fluctuations[2] have been proposed as a possible origin of the pseudogap. Alternatively, the pseudogap is attributed to a competing order such as spin density wave, charge density wave, loop current[3]. In measurements which are sensitive to the superconducting gap around the node such as Andreev reflection, penetration depth, the gap decreases with underdoping[4,5] in contrast to the pseudo-gap which increases with underdoping, suggesting a different origin of the antinodal gap from the superconducting gap. Furthermore, photoemission[6–10] and Raman[11,12] studies have indicated the presence of two distinct energy scales. In a previous paper[13], we have pointed out that the pseudo-gap shows a relatively material-independent universal behavior: the pseudo-gap size is almost the same at the same doping level while the superconducting gap is proportional to T_c, suggesting different origins for the superconducting gap and the pseudo-gap. On the other hand, a simple d-wave-like gap has been also reported in some ARPES studies[14,15]. In such a single-gap picture, the pseudogap is interpreted as a signature of preformed Cooper pairs. Thus, the discrepancy between the experimental studies has remained.

In the analysis of the STM spectra of single-layer cuprate $Bi_2Sr_2CuO_{6+\delta}$ (Bi2201), distinct behaviors of the superconducting gap and the pseudogap have been clearly demonstrated[16]. Even if the superconducting peak is not clearly observed in underdoped samples, the superconducting coherence peak has been identified by dividing the spectra in the superconducting state by the normal-state data. Also, similar analysis has been done for the ARPES spectra of Bi2201 in the anti-nodal region and a superconducting peak has been identified[17]. These results suggest that the pseudogap and the superconducting gap have distinct origins and the superconducting gap is created on top of the electronic states with relatively broad spectral features with low density of states due to the pseudogap opening. As for the single-layer cuprates $La_{2-x}Sr_xCuO_4$ (LSCO), a clear superconducting peak has been identified in the off-nodal region, however, such a clear peak has not been identified in the anti-node region[9]. In order to examine the coexistence of the superconducting gap and the pseudogap aforementioned, we have performed an ARPES study of LSCO (x=0.14, 0.10) and analyzed the spectral line shapes to extract the signature of the superconducting peak.

High-quality single crystals of LSCO (x=0.10, 0.14, 0.15) were grown by the traveling-

solvent floating-zone method. The critical temperatures of T_c's the $x = 0.10$, 0.14, and 0.15 samples were 28, 32 and 39 K, respectively. The ARPES measurements were carried out using synchrotron radiation at beamline 5-4 of Stanford Synchrotron Radiation Light Source (SSRL). We used incident photons with energies of 22 eV. SCIENTA R4000 spectrometer was used in the angle mode. The total energy resolution was about 7 meV. The samples were cleaved *in situ* and measurements were performed at 11 K ($< T_c$) and 40 K ($> T_c$).

Figure 1 shows ARPES spectra of LSCO with x=0.14 and 0.10 taken at T= 11K ($< T_c$) and T= 40K ($> T_c$). The background well away from the Fermi momenta (k_F) has been subtracted from the spectra[18]. The spectra have been divided by a convoluted Fermi-Dirac function. One can clearly see that the superconducting gap for the x=0.14 sample in the off-nodal region opens below T_c [panel (a1)] and closes above T_c [panel (a2)]. The spectra for the x=0.10 sample also shows a similar trend but the gap opens even above T_c as shown in panel (c2), suggestive of a pseudogap opening. In the anti-node region, in contrast, spectral weight near E_F is strongly suppressed even above T_c [(b2) and (d2)], indicating a pseudogap behavior. The difference between the spectra below and above T_c is not apparent. From these data, we derive the energy of the superconducting peak as described below.

In order to identify fine structures associated with the superconducting transition, we have applied a similar analysis to that employed in the previous STM[16] and ARPES studies[19] as described in Figs. 2 (a1) -(a3). First, integrated spectrum along cut b in Fig. 1[panel (a1)] is divided by Fermi-Dirac function convoluted by the energy resolution [panel (a2)]. Then, the spectrum below T_c is divided by that above T_c [panel (a3)]. As a result, we have obtained a peak-gap structure near E_F even in the anti-nodal region where the pseudo-gap dominates the spectra, indicating superconducting peak and gap. In the same manner, the various cuts shown in Fig. 1 have been analyzed and the results are shown in Fig. 2 (b1)-(c2). Note that the obtained spectra is analogous to the tunneling spectra of s-wave superconductors[20] because the superconducting order parameter is approximately constant around k_F on a single cut.

Strictly speaking, the division by a convoluted Fermi-Dirac function is an approximate method to determine the gap size and one cannot exclude spurious effect due to the finite energy resolution. In order to determine the superconducting gap energy more precisely, we performed deconvolution to remove the experimental energy resolution from the cut-integrated spectra using the maximum entropy method (MEM)[21] [Fig. 3(a1)]. Then, the

spectra were divided by the Fermi-Dirac function [Fig. 3(a2)]. Finally, the spectra below T_c were divided by those above T_c [Fig. 3(a3)]. In Fig. 3, we compare the processed spectra with [panels (c1) and (c2)] and without deconvolution [panels (b1) and (b2)]. Also, we have shown processed spectra (without deconvolution) for x=0.15 near the node taken by the laser ARPES with a high resolution of $\sim$ 2.8 meV [Fig. 3(d)]. The peak energies are plotted as a function of the d-wave parameter $(\cos(k_x) - \cos(k_y))/2$ in panel (e) and compared with the previous result of x=0.15 which shows "two-gap" behavior[13]. Note that the peak positions of the deconvoluted spectra are closer to E_F by $\sim$ 5meV than those without deconvolution, nearly follows the pure d-wave from the nodal to the anti-nodal regions[13]. Furthermore, the gap sizes in the off-nodal region for both the x=0.14 and 0.10 samples are almost the same, in contrast to the previous ARPES study of LSCO[22]. The observed d-wave-like gap in the anti-node region Δ_0 $\sim$12-14 meV gives a strong coupling ratio $2\Delta_0/k_BT_c \sim 10$, similar to the previous Bi2201 result[17]. The nearly constant Δ_0 from the optimally doped to underdoped regions is consistent with the recent results in $Bi_2Sr_2CaCu_2O_{8+\delta}$ (Bi2212)[23] with larger $T_c >$ 90 K, indicating universal behavior in the high-T_c cuprates.

Here, we shall discuss differences in the "two-gap" behavior between the single-layer and bi-layer cuprates. In the single-layer cuprates such as LSCO and Bi2201, the co-existence of the pseudogap and the superconducting peak in the anti-nodal direction has been revealed by the ARPES[19] and STM studies[24,25] including the present result. However, in the case of Bi2212[6,7], such two energy scales have not been resolved in the anti-nodal spectra. Only a single-peak structure appears below T_c in the optimally-doped and under-doped regions. The different behaviors between the single- and double-layer cuprates can be understood as follows: When the pseudogap has a different origin from the superconducting gap, the superconducting peak is created on the pseudogap feature of the broad incoherent spectral weight.

Figure 4 shows the doping dependences of Δ^*, Δ_0 and T^* for LSCO and Bi2201 as well as those for double-layer Bi2212 (inset). Here, antinodal gap Δ^* is defined by the peak energy in the antinodal region[13] and T^* is the pseudogap temperature. As shown in the figure, in the single-layer cuprates, which have relatively low T_c's, the energy scale of the superconducting gap is smaller than that of the pseudogap and the T_c is lower than the pseudogap temperature T^* in the optimally-doped and the underdoped region. Therefore, the superconducting gap appears below T_c within the pseudogap which is created below

T^*, resulting in the two energy scales in the spectral weight distribution. On the other hand, in the bi-layer cuprates Bi2212, which has a relatively high T_c comparable to T^*, both energy scales are comparable and T_c and T^* are also comparable in the optimally doped region [Fig.4(inset)]. Because the pseudogap has a comparable energy scale with the superconducting gap Δ_0 and opens at nearly the same temperatures, the two gaps cannot be clearly resolved. Thus, the superconducting peak may show only a weak deviation from the pure d-wave in Bi2212[6,7], unlike the strong deviation with two-energy scales in the single-layer cuprates[8,9,13].

The present study has revealed that the superconducting gap has nearly pure d-wave form and exists even in the anti-node direction in the optimally-doped to underdoped region. A phenomenological model for the two gap state proposed by Yang, Rice and Zhang (YRZ) well accords with the present coexistence of the superconducting and the pseudogap[26]. While YRZ assumes a RVB gap as the anti-nodal gap, there are several possible candidates for the origin of the pseudogap. Calculations assuming an order parameter different from the superconductivity such as valence bond glass[27] and spin-density wave (SDW) state[28] have predicted that the superconducting gap persists beyond the end of the Fermi arc all the way to the antinode. In accordance with the present observation. Particularly, in the SDW-based calculation[28], a hump-like pseudogap and a sharp superconducting peak in the anti-node direction as seen in the present result have been reproduced. A temperature dependent ARPES study reveals particle-hole asymmetry of the anti-node gap, most likely due to the density-wave gap formation[29]. This observation would be related to the charge ordered state observed in STM[30] or stripe formation[31]. From STM results of the charge order[24,32], the pseudogap in the anti-nodal region is most likely to link to such a two-dimensional electronic charge order.

In conclusion, we have identified the superconducting peak LSCO (x=0.10, 0.14) in the anti-nodal region from analysis of the ARPES spectra above and below T_c. The superconducting peaks follow the pure d-wave on top of the pseudogap of a larger energy scalle. The d-wave gap parameter Δ_0 of the optimally and underdoped samples are nearly the same similar to the Bi2212 results[23], indicating universal behavior in the high-T_c cuprates. Since the superconducting order parameter is nearly doping independent in the underdoped region, the drop of T_c with underdoping is due to the decreasing length of Fermi arc. The present results have reinforced that the pseudogap and the superconducting gap are distinct

phenomena.

We are grateful to H. Ding for informative discussions. This work was supported by a Grant-in-Aid for Young Scientists (B) and the Japan-China-Korea A3 Foresight Program from the Japan Society for the Promotion of Science. SSRL is operated by the Department of Energy's Office of Basic Energy Science, Division of Chemical Sciences and Material Sciences.

---

[1] J. V. Emery and S. A. Kivelson, Nature **374**, 434 (1998).

[2] J. R. Engelbrecht, A. Nazarenko, M. Randeria, and E. Dagotto, Phys. Rev. B **57**, 13406 (1998).

[3] M. E. Simon and C. M. Varma, Phys. Rev. Lett. **89**, 247003 (2002).

[4] G. Deustcher, Nature **397**, 410 (1999).

[5] C. Panagopoulos, J. R. Cooper, and T. Xiang, Phys. Rev. B **57**, 13422 (1998).

[6] K. Tanaka, W. S. Lee, D. H. Lu, A. Fujimori, T. Fujii, Risdiana, I. Terasaki, D. J. Scalapino, T. P. Devereaux, Z. Hussain, and Z.-X. Shen, Science **314**, 1910 (2006).

[7] W. S. Lee, I. M. Vishik, K. Tanaka, D. H. Lu, T. Sasagawa, N. Nagaosa, T. P. Devereaux, Z. Hussain, and Z.-X. Shen, Nature **450**, 81 (2007).

[8] T. Kondo, T. Takeuchi, A. Kaminski, S. Tsuda, and S. Shin, Phys. Rev. Lett. **98**, 267004 (2007).

[9] K. Terashima, H. Matsui, T. Sato, T. Takahashi, M. Kofu, and K. Hirota, Phys. Rev. Lett. **99**, 017003 (2007).

[10] M. Hashimoto, T. Yoshida, K. Tanaka, A. Fujimori, M. Okusawa, S. Wakimoto, K. Yamada, T. Kakeshita, H. Eisaki, and S. Uchida, Phys. Rev. B **75**, 140503(R) (2007).

[11] M. Opel, R. Nemetschek, C. Hoffmann, R. Philipp, P. F. Müller, R. Hackl, I. Tüttö, A. Erb, B. Revaz, E. Walker, H. Berger, and L. Forró, Phys. Rev. B **61**, 9752 (2000).

[12] M. L. Tacon, A. Sacuto, A. Georges, G. Kotliar, Y. Gallais, D. Colson, and A. Forget, Nature Physics **2**, 537 (2006).

[13] T. Yoshida, M. Hashimoto, S. Ideta, A. Fujimori, K. Tanaka, N. Mannella, Z. Hussain, Z.-X. Shen, M. Kubota, K. Ono, S. Komiya, Y. Ando, H. Eisaki, and S. Uchida, Phys. Rev. Lett. **103**, 037004 (2009).

[14] J. Meng, W. Zhang, G. Liu, L. Zhao, H. Liu, X. Jia, W. Lu, X. Dong, G. Wang, H. Zhang, Y. Zhou, Y. Zhu, X. Wang, Z. Zhao, Z. Xu, C. Chen, and X. J. Zhou, Phys. Rev. B **79**, 024514

(2009).

[15] M. Shi, A. Bendounan, E. Razzoli, S. Rosenkranz, M. R. Norman, J. C. Campuzano, J. Chang, M. Mansson, Y. Sassa, T. Claesson, O. Tjernberg, L. Patthey, N. Momono, M. Oda, M. Ido, S. Guerrero, C. Mudry, and J. Mesot, Europhys. Lett. **88**, 27008 (2009).

[16] M. C. Boyer, W. D. Wise, K. Chatterjee, M. Yi, T. Kondo, T. Takeuchi, H. Ikuta, and E. W. Hudson, Nature Physics **3**, 802 (2007).

[17] J.-H. Ma, Z.-H. Pan, F. C. Niestemski, M. Neupane, Y.-M. Xu, P. Richard, K. Nakayama, T. Sato, T. Takahashi, H.-Q. Luo, L. Fang, H.-H. Wen, Z. Wang, H. Ding, and V. Madhavan, Phys. Rev. Lett. **101**, 207002 (2008).

[18] M. Hashimoto, R.-H. He, I. M. Vishik, F. Schmitt, R. G. Moore, D. H. Lu, Y. Yoshida, H. Eisaki, Z. Hussain, T. P. Devereaux, and Z.-X. Shen, Phys. Rev. B **86**, 094504 (2012).

[19] H. Ding, J. R. Engelbrecht, Z. Wang, J. C. Campuzano, S.-C. Wang, H.-B. Yang, R. Rogan, T. Takahashi, K. Kadowaki, and D. G. Hinks, Phys. Rev. Lett. **87**, 227001 (2001).

[20] W. L. McMillan and J. M. Rowell, Phys. Rev. Lett. **14**, 108 (1965).

[21] The MEM has been used to numerically deconvolute an image or spectrum which has been convoluted by some function. In the deconvolution process, the generalized entropy is defined in order to overcome the numerical instability. In previous ARPES studies, the Eliashberg function has been extracted from the ARPES data by the MEM[33,34].

[22] M. Shi, J. Chang, S. Pailhés, M. R. Norman, J. C. Campuzano, M. Månsson, T. Claesson, O. Tjernberg, A. Bendounan, L. Patthey, N. Momono, M. Oda, M. Ido, C. Mudry, and J. Mesot, Phys. Rev. Lett. **101**, 047002 (2008).

[23] I. M. Vishik, M. Hashimoto, R.-H. He, W.-S. Lee, F. Schmitt, D. Lu, R. G. Moore, C. Zhang, W. Meevasana, T. Sasagawa, S. Uchida, K. Fujita, S. Ishida, M. Ishikado, Y. Yoshida, H. Eisaki, Z. Hussain, T. P. Devereaux, and Z.-X. Shen, PNAS **109**, 18332 (2012).

[24] T. Kurosawa, T. Yoneyama, Y. Takano, M. Hagiwara, R. Inoue, N. Hagiwara, K. Kurusu, K. Takeyama, N. Momono, M. Oda, and M. Ido, Phys. Rev. B **81**, 094519 (2010).

[25] Y. He, Y. Yin, M. Zech, A. Soumyanarayanan, M. M. Yee, T. Williams, M. C. Boyer, K. Chatterjee, W. D. Wise, I. Zeljkovic, T. Kondo, T. Takeuchi, H. Ikuta, P. Mistark, R. S. Markiewicz, A. Bansil, S. Sachdev, E. W. Hudson, and J. E. Hoffman, Science **344**, 608 (2014).

[26] K.-Y. Yang, T. M. Rice, and F.-C. Zhang, Phys. Rev. B **73**, 174501 (2006).

[27] L. R. Niestemski and Z. Wang, Phys. Rev. Lett. **102**, 107001 (2009).

[28] T. Das, R. S. Markiewicz, and A. Bansil, Phys. Rev. B **77**, 134516 (2008).

[29] M. Hashimoto, R.-H. He, K. Tanaka, J.-P. Testaud, W. Meevasana, R. G. Moore, D. Lu, H. Yao, Y. Yoshida, H. Eisaki, T. P. Devereaux, Z. Hussain, and Z.-X. Shen, Nature Physics **6**, 414 (2010).

[30] T. Hanaguri, C. Lupien, Y. Kohsaka, D.-H. Lee, M. Azuma, M. Takano, H. Takagi, and J. C. Davis, Nature **430**, 1001 (2004).

[31] J. M. Tranquada, B. J. Sternlieb, J. D. Axe, Y. Nakamura, and S. Uchida, Nature **375**, 561 (1995).

[32] E. H. da Silva Neto, P. Aynajian, A. Frano, R. Comin, E. Schierle, E. Weschke, A. Gyenis, J. Wen, J. Schneeloch, Z. Xu, S. Ono, G. Gu, M. Le Tacon, and A. Yazdani, Science **343**, 393 (2014).

[33] J. Shi, S.-J. Tang, B. Wu, P. T. Sprunger, W. L. Yang, V. Brouet, X. J. Zhou, Z. Hussain, Z.-X. Shen, Z. Zhang, and E. W. Plummer, Phys. Rev. Lett. **92**, 186401 (2004).

[34] X. J. Zhou, J. Shi, T. Yoshida, T. Cuk, W. L. Yang, V. Brouet, J. Nakamura, N. Mannella, S. Komiya, Y. Ando, F. Zhou, W. X. Ti, J. W. Xiong, Z. X. Zhao, T. Sasagawa, T. Kakeshita, H. Eisaki, S. Uchida, A. Fujimori, Z. Zhang, E. W. Plummer, R. B. Laughlin, Z. Hussain, and Z.-X. Shen, Phys. Rev. Lett. **95**, 117001 (2005).

[35] S.-i. Ideta, T. Yoshida, A. Fujimori, H. Anzai, T. Fujita, A. Ino, M. Arita, H. Namatame, M. Taniguchi, Z.-X. Shen, K. Takashima, K. Kojima, and S.-i. Uchida, Phys. Rev. B **85**, 104515 (2012).

[36] T. Yoshida, M. Hashimoto, I. M. Vishik, Z.-X. Shen, and A. Fujimori, J. Phys. Soc. Jpn. **81**, 011006 (2012).

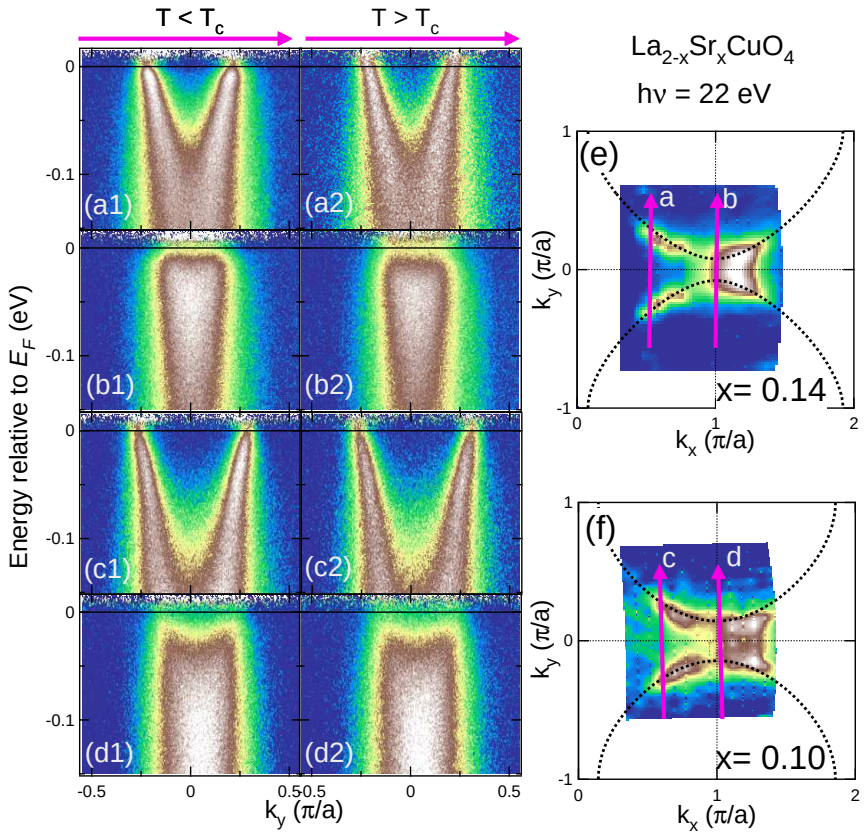

FIG. 1. (Color online) ARPES spectra of LSCO with x=0.14 and 0.10. (a1)-(d2) ARPES intensity plots correspond to cuts a-d in panels (e) and (f). The data in the left (right) have been measured below (above) T_c. Spectra have been divided by the Fermi-Dirac function convoluted with the energy resolution function. (e)(f) Intensity at E_F mapped in the k_x-k_y plane. Dotted lines illustrate Fermi surfaces.

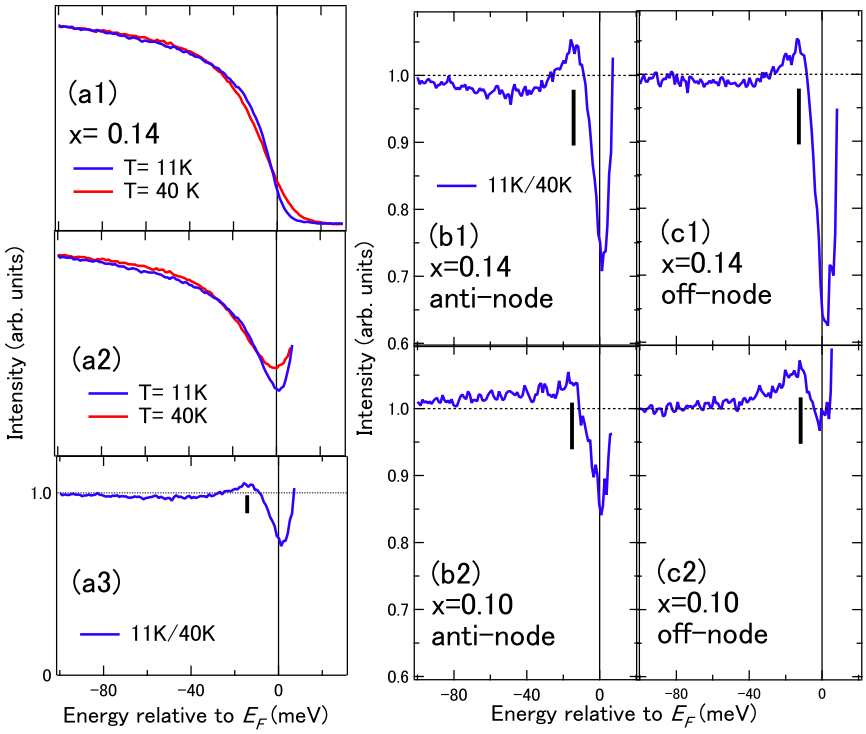

FIG. 2. (Color online) Superconducting peaks observed in the ARPES spectra of LSCO with x=0.14 and 0.10. (a1) Cut-integrated spectra for x=0.14 for cut b in Fig.1 (e). (a2) Spectra in panel (a1) have been divided by the Fermi function convoluted with the energy resolution function. (a3) Spectra below T_c in panel (a2) have been divided by that above T_c. (b1)-(c2) Spectra corresponding to cuts in Fig. 1 after above processing. Vertical bars indicate the peak positions.

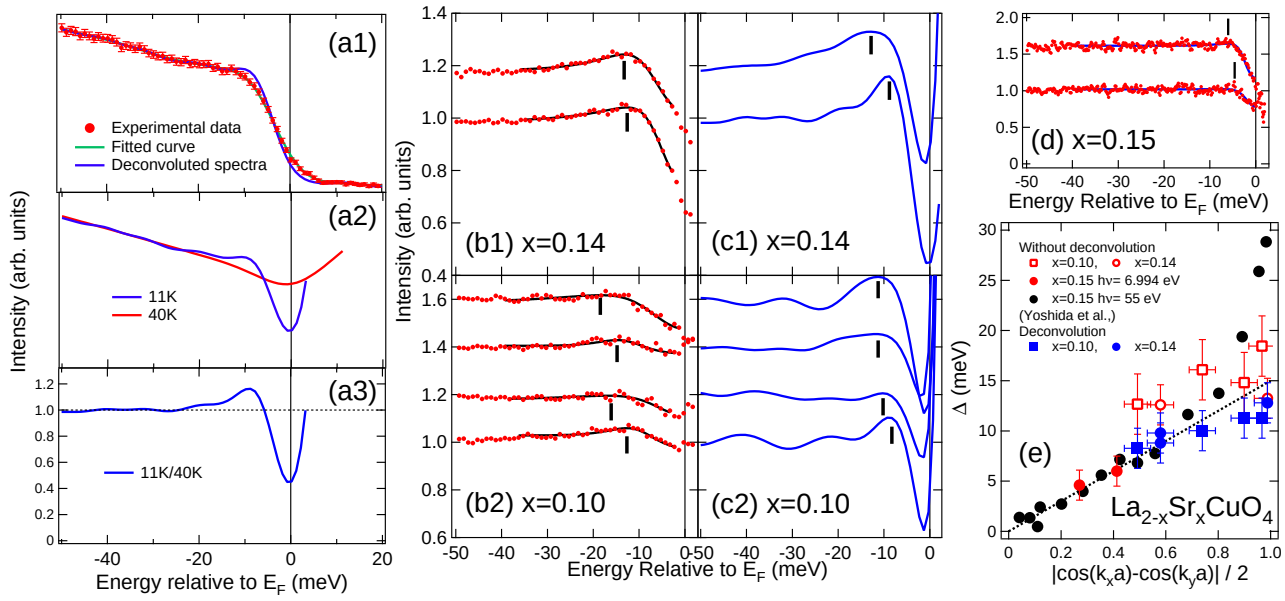

FIG. 3. (Color online) Angular dependence of the superconducting peaks obtained from ARPES spectra of LSCO with x=0.14 and 0.10. (a1) Cut-integrated spectrum for x=0.14 in the off-nodal direction taken at 11 K and its deconvoluted spectrum using the MEM. Fitted curve produced by the MEM well reproduce the original experimental data. (a2) Deconvoluted spectra divided by the Fermi-Dirac function. (a3) Spectrum obtained by dividing the 11K data ($< T_c$) by the 40K data ($> T_c$)in panel (a2). (b1)(b2) Superconducting peak obtained in Fig.2 (c1)(c2). The spectra in panels (b1) and (b2) have been deconvoluted with the energy resolution using the MEM. (d) Superconducting gap near the nodal direction for x=0.15 taken at $h\nu$=6.994 eV using a UV laser at the Institute of Solid State Physics (ISSP), the University of Tokyo. The data was analyzed in the same manner as in panels (b1) and (b2). (e) Angular dependence of the superconducting peak are plotted as a function of d-wave parameter $|\cos(k_x) - \cos(k_y)|/2$. For comparison, previous results of the gap for x=0.15 are also plotted.

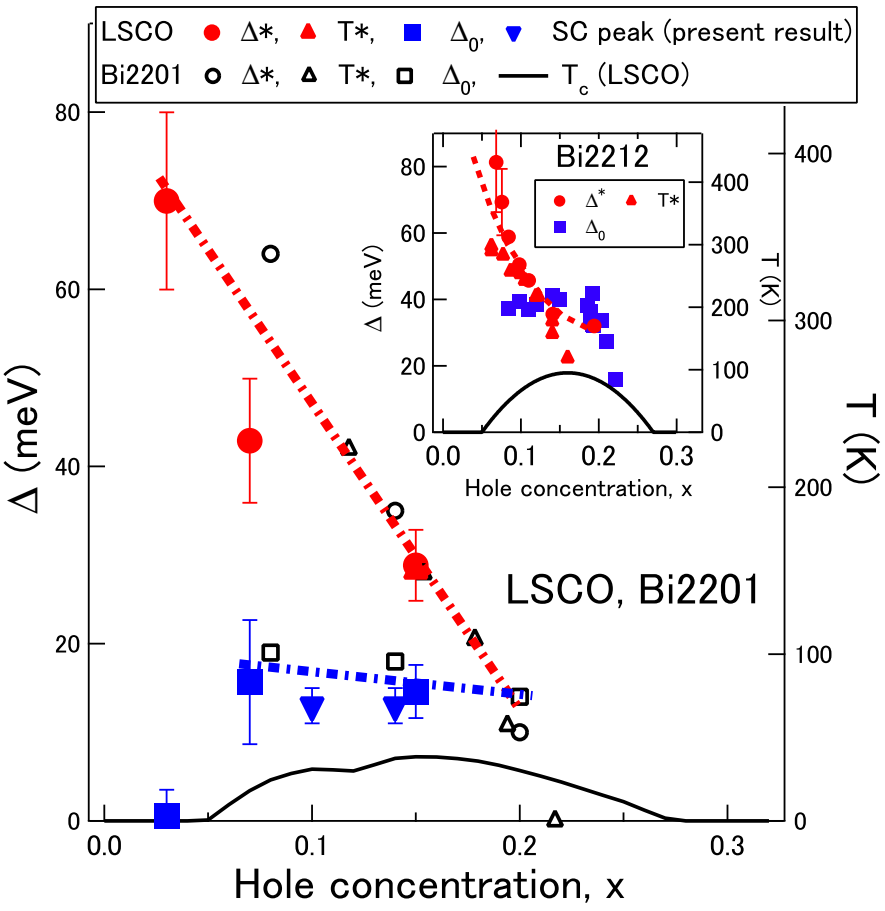

FIG. 4. (Color online) Doping dependences of the characteristic energies (Δ^*, Δ_0 Refs.13, 35, and 36) and temperatures (T^*, T_c) for the single-layer cuprates (LSCO, Bi2201). Anti-nodal gap Δ^* is defined by the energy of hump or peak in the anti-nodal region[36]. Parameter values have been taken from Ref.36 and references therein. The present LSCO result of the SC peak energy in the antinode direction is also plotted. Inset shows those for the double-layer cuprates Bi2212. Gap energies Δ and temperatures T have been scaled as $2\Delta = 4.3k_BT$ in these plots.